J. Phys. Chem. A **2008,** *112,* 8929–8937

Density Functional Theory Study of the Adsorption of Formaldehyde on Pd_4 and on $Pd_4/\gamma\text{-}Al_2O_3$ Clusters[†]

José Walkimar de M. Carneiro*,[‡],[§] and Maurício T. de M. Cruz[§]

Departamento de Química Inorgânica, and Pós-Graduação em Química Orgânica, Instituto de Química, Universidade Federal Fluminense, Outeiro de São João Batista, s/n, 24020-141 Niterói - RJ, Brazil

Received: February 22, 2008; Revised Manuscript Received: June 3, 2008

B3LYP/LANL2DZ and B3LYP/6-31G(d)-restricted and -unrestricted calculations are employed to calculate energies and adsorption forms of formaldehyde adsorbed on planar and on tetrahedral Pd_4 clusters and on a Pd_4 cluster supported on $Al_{10}O_{15}$. Formaldehyde adsorbs on planar Pd_4 in the η^2(C,O)−di-σ adsorption mode, while on tetrahedral Pd_4, it adsorbs in the η^2(C,O)−π adsorption mode. The adsorption energy on planar Pd_4 is −21.4 kcal·mol^{-1}, whereas for the tetrahedral Pd_4 cluster, the adsorption energy is −13.2 kcal·mol^{-1}. The latter value is close to experimental findings (−12 to −14 kcal·mol^{-1}). Adsorption of formaldehyde on Pd_4 supported on an $Al_{10}O_{15}$ cluster leads essentially to the same result as that found for adsorption on the tetrahedral Pd_4 cluster. Charge density analysis for the interaction between formaldehyde and the Pd_4 clusters indicates strong backdonation in the η^2 adsorption mode, leading to positive charge on the Pd_4 cluster. NBO analysis shows that the highly coordinated octahedral aluminum atoms of $Al_{10}O_{15}$ donate electron density to the supported Pd_4 cluster, while tetrahedral aluminum atoms with lower coordination number have acidic nature and therefore act as electron acceptors.

Introduction

Supported metal particles are commonly used as heterogeneous catalysts. The active catalytic material is usually dispersed on the support as small particles in order to maximize surface area.[1] Although the active site is usually represented by the metal surface, the support also plays a relevant role in the reactivity of the supported metal.[2−6] For example, the hydrogenation of propylene is faster on $Ir_4/\gamma\text{-}Al_2O_3$ than that on Ir_4/MgO.[7] Similarly, the adsorption of CO on supported palladium is stronger when the TiO_2 and the Al_2O_3 oxides are used as a support, as compared to the SiO_2 oxide.[8] In the present paper, we report DFT B3LYP calculations concerning the effect of $\gamma\text{-}Al_2O_3$ on the adsorption of formaldehyde on a small palladium cluster. Although the size of metal particles on a support may vary to some degree, dispersed clusters are usually formed by a small number of atoms. Analysis of a fresh platinum catalyst supported on Al_2O_3 determined an average Pt−Pt coordination number of 2.6, suggesting a platinum cluster size of 3−4 atoms dispersed on the γ-alumina surface.[9]

Palladium particles supported on $\gamma\text{-}Al_2O_3$ are among the most usual heterogeneous catalytic systems available. Although several studies report on the adsorption properties of $\gamma\text{-}Al_2O_3$, especially for the adsorption of alkanes,[10−14] theoretical simulations of the effect of the $\gamma\text{-}Al_2O_3$ support on the adsorption features of palladium are still scarce. Alumina, mainly as $\gamma\text{-}Al_2O_3$, has been widely used as an active catalytic support,[15] primarily due to its large specific surface area. Structural models for the active surface of γ-alumina were suggested.[16−18] The active (110C) surface exhibits hollow sites with nonequivalent tetrahedral and octahedral aluminum ions, which are most probably responsible for adsorption.[19] The Pd−Al_2O_3 interactions result in charge transfer from the aluminum cations to the deposited Pd atoms.[20−23] Supercell DFT calculations on the Pd/$\gamma\text{-}Al_2O_3$ (110C) interface at low coverage[24] indicate strong adsorption on tetrahedral Al sites and weaker interaction with the octahedral Al sites. In any case, the acid properties of the cationic sites dominate and determine the initial steps of the adsorbate−support interface interactions.

Formaldehyde may adsorb on transition metals in two bonding modes, η^1−(O) and η^2−(C,O) or the top−bridge−top mode (tbt structure).[25] In the η^1−(O) configuration, the molecule binds to the surface via the oxygen atom using one of its lone pairs. In the η^2−(C,O) mode, the adsorbate interacts with the substrate via both the carbon and the oxygen atoms. Additionally, there may be two η^2−(C,O) adsorption modes. Bonding of the carbon and oxygen atoms to contiguous active sites leads to σ-type bonding arrangements, resulting in an η^2−(C,O)−di-σ adsorption mode. In contrast, when the carbon and oxygen atoms both bind to the same active site, they form π-type bonding arrangements, leading to an η^2−(C,O)−π adsorption form (Figure 1). On clean surfaces of group VIII metals, the η^2−(C,O) mode is preferred,[25] although both adsorption forms have been detected experimentally. Previous experimental and theoretical studies on adsorption of formaldehyde on the transition-metal Pd(111), Cu(111), and Pt(111) surfaces indicate that the η^2−(C,O) adsorption geometry (i.e., interaction of both the oxygen and carbon atoms with the surface) is the most likely.[26−36] Temperature-programmed desorption experiments[34] as well as results of slab model calculations point to the η^2 form as the most probable, with an adsorption energy in the range of 12−14.6 kcal·mol^{-1}.[34,35] In cluster calculations using Pd_8 and Pd_{19} models of the Pd(111) surface, the η^2−(C,O) adsorption mode is preferential.[31] Slab model density functional investigations exclusively reported the η^2−(C,O) adsorption form as the most stable.[30,32]

[†] Part of the special section for the "Symposium on Energetics and Dynamics of Molecules, Solids and Surfaces".

* To whom correspondence should be addressed. E-mail: walk@vm.uff.br.

[‡] Departamento de Química Inorgânica.

[§] Pós-Graduação em Química Orgânica.

10.1021/jp801591z CCC: \$40.75

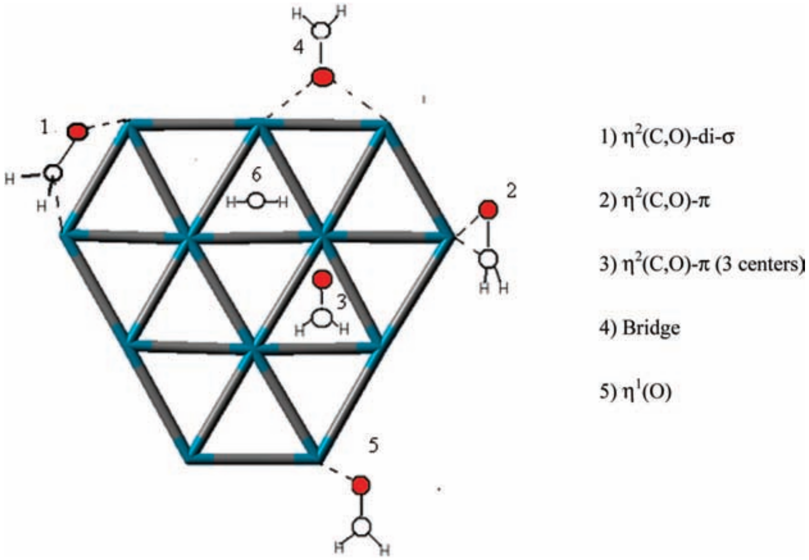

Figure 1. Different forms for interactions of formaldehyde with the palladium(111) surface.

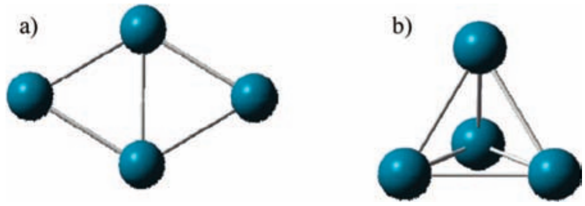

Figure 2. (a) Planar and (b) tetrahedral Pd_4 clusters.

Computational Methods

In the present work, we report data for formaldehyde adsorption on models of the (111) surface of palladium and of palladium supported on the (110C) surface of γ-Al_2O_3 using the cluster model approach. The bulk palladium metal has a face-centered cubic (fcc) crystal structure.[37] On the basis of this structure, the (111) palladium surface was modeled by two clusters, both containing four palladium atoms, (i) a planar rhombohedral arrangement in D_{2h} symmetry and (ii) a tetrahedral arrangement in T_d symmetry, as shown in Figure 2. These clusters form a compact section of the (111) fcc ideal palladium surface. Small cluster models have proved useful in the study of the adsorption of individual species and have provided accurate descriptions of adsorbate structures, vibrations, and chemisorption energies.[38−41] The formaldehyde molecule was fully optimized on both palladium clusters, while simultaneously keeping the Pd−Pd distances fixed at the bulk Pd−Pd value of 2.751 Å.[37] When possible, symmetry was imposed. The adsorption energy (E_{ad}) corresponds to the energy difference between the H_2CO/Pd_4 complex and its components (H_2CO and Pd_4) at infinite separation and is calculated according to eq 1

$$E_{ad} = E_{(H2CO/Pd4)} - [E_{(H2CO)} + E_{(Pd4)}] \tag{1}$$

All calculations were done with the B3LYP hybrid functional as proposed and parametrized by Becke.[42] This is a mixture of Hartree−Fock and DFT exchange terms with the gradient-corrected correlation functional of Lee et al.[43] As a first approach, the metal atoms were described by the LANL2DZ pseudopotential[44] and its accompanying D95V basis set for the valence electrons, which, in the case of palladium, includes the outer 18 electrons. For the nonmetallic atoms (oxygen, carbon, and hydrogen in the present case), the valence double-ζ basis set of Dunning and Huzinaga (D95V)[45] was employed. The combination (B3LYP/LANL2DZ) was employed to calculate the energy of the bare clusters and to optimize the geometry of formaldehyde interacting with the fixed clusters. For each optimized geometry, the energy was refined through single-point energy calculations, now replacing the D95V basis set on carbon, oxygen, and hydrogen atoms with the 6-31G(d) basis set[46] while maintaining the LANL2DZ pseudopotential for the metal atoms.

As a second step, the same B3LYP/LANL2DZ combination was employed to calculate the adsorption energies of formaldehyde over the Pd_4 cluster, now, however, in the presence of an alumina cluster. For these calculations, we used a γ-Al_2O_3(110C) surface modeled with 18 aluminum and 27 oxygen atoms, as shown in Figure 3. The (110C) alumina face was chosen because, in addition to being the most stable, it also exposes both tetrahedral and octahedral aluminum atoms as well as oxide anions.[24,47] Such a cluster was designed in order to represent a small slice of the bulk γ-alumina and was built using experimental parameters for the bulk γ-alumina.[48,49] One Pd_4 cluster with Pd−Pd distances of 2.751 Å was then deposited on the top of the (110C) face of the $Al_{18}O_{27}$ cluster, and its geometry was fully optimized. During the optimization of the $Pd_4/Al_{18}O_{27}$ ensemble, only the palladium atoms were allowed to fully relax. Several adsorption positions of formaldehyde on the $Pd_4/Al_{18}O_{27}$ ensemble are possible. In order to reduce computational cost in the determination of the best position for formaldehyde adsorption on the Pd/alumina surface, the size of the alumina cluster was reduced. The two layers of the $Al_{18}O_{27}$ cluster farther from the adsorption interface were removed, reducing the $Pd_4/Al_{18}O_{27}$ to a $Pd_4/Al_{10}O_{15}$ ensemble. To test the quality of this reduced model, one CO molecule was adsorbed on various positions on the $Pd_4/Al_{10}O_{15}$ surface, and the preferential adsorption forms with their respective energies were compared with experimental data.[50] The calculated higher adsorption energy (-53.1 kcal·mol^{-1}) is close to the calorimetric experimental adsorption energy (-47.8 kcal·mol^{-1}),[50] giving support to our model. In addition, one calculation of formaldehyde adsorption considering the larger Al_2O_3 model ($Al_{18}O_{27}$) reduces the adsorption energy by only 2 kcal·mol^{-1}. After model validation, the formaldehyde molecule was adsorbed on several positions of the $Pd_4/Al_{10}O_{15}$ ensemble. In this case, the geometry of formaldehyde was

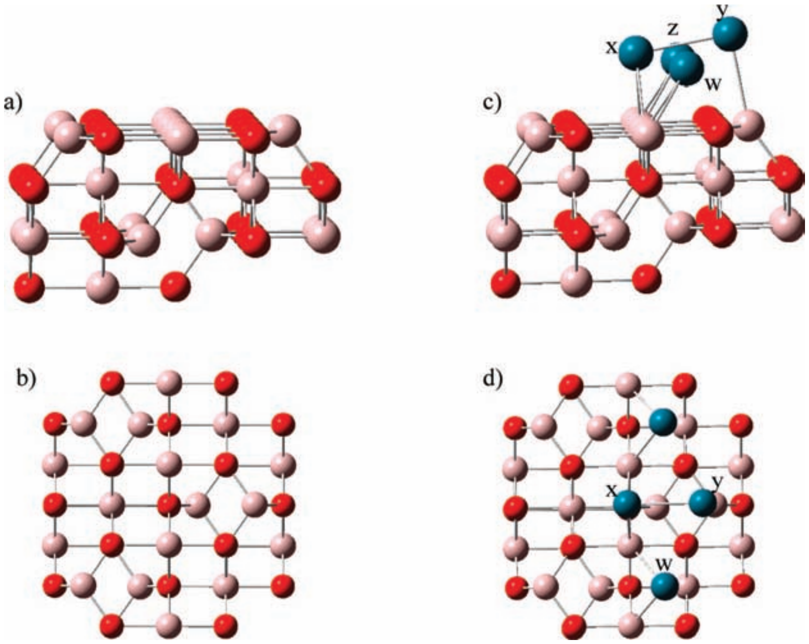

Figure 3. Lateral (a) and top (b) view of the $Al_{18}O_{27}$ cluster. Lateral (c) and top (d) view of the $Pd_4/Al_{18}O_{27}$ complex; x, y, w, and z denote the palladium atoms (see text).

allowed to fully relax while maintaining the geometry of the $Pd_4/Al_{10}O_{15}$ fixed at the previously optimized arrangement.

Adsorption energies were computed as before by subtracting the energies of the isolated formaldehyde molecule and the $Pd_4/Al_{10}O_{15}$ cluster from the energy of the $H_2CO/Pd_4/Al_{10}O_{15}$ system, according to eq 2

$$E_{\mathrm{ad}} = E_{(\mathrm{H2CO/Pd4/Al10O15})} - [E_{(\mathrm{H2CO})} + E_{(\mathrm{Pd4/Al10O15})}] \quad (2)$$

A negative value for the adsorption energy means that the corresponding adsorbed state is thermodynamically more stable than the unbounded state.

The calculations described above were carried out using the restricted formalism in the singlet electronic spin state. This was done considering the $4d^{10}$ closed-shell electronic ground-state configuration for the palladium atom. However, as recently shown,[51] the ground electronic state for small Pd_7 and Pd_{10} clusters have triplet ($S = 1$) and septet ($S = 3$) spin states, respectively. This prompted us to redo the above calculations considering the several possible electronic spin states. Therefore, the geometry of formaldehyde interacting with both the Pd_4 clusters and the $Pd_4/Al_{10}O_{15}$ ensemble was reoptimized using the unrestricted formalism considering the electronic spin states' triplet ($S = 1$), quintet ($S = 2$), septet ($S = 3$), and nonet ($S = 4$). For the unrestricted calculations, the stability of the final wave function was tested. The reported adsorption energy in each case is that found with the most stable wave function using the bigger basis set.

In order to determine the effect of the support on the properties of the palladium clusters, we focused on the electrostatic potential (ESP)-derived charges, using the Merz−Kollman−Singh scheme (MKS population analysis), which fits the ESP to points selected on a set of concentric spheres around each atom.[52,53] In the MKS scheme, the charge transfer and electrostatic components do not have the usual physical meanings considered in the Mulliken and Morokuma analyses.[54,55] Additionally, a set of natural bond orbital (NBO) calculations were carried out in order to evaluate the nature of the electronic interactions between the formaldehyde/Pd and Pd/Al_2O_3 interfaces. All calculations were performed using the Gaussian 03W computational package.[56]

Results

Adsorption of Formaldehyde on Pd_4. Two Pd_4 clusters were tested, one planar rhombohedral in D_{2h} symmetry and another tetrahedral in T_d symmetry (Figure 2). For the planar Pd_4 arrangement, the most stable spin state is singlet, while for the tetrahedral arrangement, the triplet spin state is the most stable. Previous calculations on Pd_4 clusters consistently reported the tetrahedral arrangement as the most stable when compared to either linear, squared, or rhombohedral arrangements.[57,58] For the tetrahedral cluster, the triplet spin state has been found as the most stable,[6,59−62] although in some studies, the singlet state was found almost degenerated.[63,64] In our studies, the tetrahedral arrangement is considerably more stable than the planar arrangement (by 22.0 $\mathrm{kcal \cdot mol^{-1}}$). When interacting with the Al_2O_3 surface, the most stable arrangement for Pd_4 is an distorted intermediate structure between the planar and the tetrahedral forms. In the distorted structure, the quintet spin state is the most stable, probably due to the more dispersed arrangement of the palladium atoms over the Al_2O_3 surface. DFT calculations using the plane-wave basis set for the Pd_4 cluster supported on the (100) and (110) γ-alumina surface found the triplet state as the most stable, even though the energy difference for lower spin state was small.[65]

Figure 1 shows possible adsorption modes of formaldehyde on the (111) face of palladium. When considering the planar Pd_4 cluster, the arrangements given in Figure 4 were found. The η^2−(C,O) adsorption forms A and C, with di-σ geometry, are those which give the higher (more negative) adsorption energy (A = −21.4 $\mathrm{kcal \cdot mol^{-1}}$; C = −20.2 $\mathrm{kcal \cdot mol^{-1}}$, Table 1). These are the structures where formaldehyde interacts with two palladium atoms of the border of the cluster. Previous calculations[27] as well as experimental[34] results also reported the η^2(C,O) form as the preferential one, with two typical σ interactions between the formaldehyde and the palladium cluster. The other adsorption forms (η^2(C,O)−di-σ (form B); η^2(C,O)−π (form D), η^2(C,O)−π (three-center) (form E); and η^1(O) (form

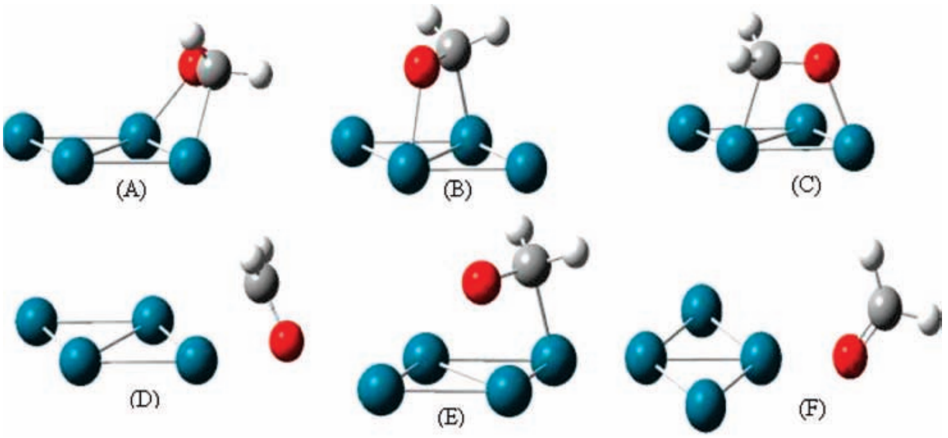

Figure 4. Adsorption forms for formaldehyde adsorption on a planar Pd_4 cluster.

TABLE 1: Adsorption Energy (E_{ad}, kcal·mol^{-1}), Charge Density on Pd_4 (q_t), and Selected Geometrical Parameters for Formaldehyde Adsorbed on Planar Pd_4 (distances in angstroms and bond angles and dihedral angles in degrees)

	A	B	C	D	E	F
C−Pd	2.055	2.048	2.051	2.180	2.056	3.114
O−Pd	2.004	1.977	1.990	2.158	2.241	2.133
C−O	1.358	1.386	1.374	1.316	1.379	1.252
C−H	1.102	1.104	1.103	1.098	1.102	1.098
H−C−O	115.918	113.626	114.156	120.058	114.572	121.793
H−C−O−H	20.630	22.786	21.691	9.724	21.666	0.000
E_{ad}[a]	−21.40	−15.50	−20.19	−16.28	−7.06	−10.91
q_t (Pd)	+0.152	+0.145	+0.144	+0.072	+0.115	−0.133

[a] Adsorption energies were calculated for the triplet state for all adsorption forms but B, for which the singlet state was used.

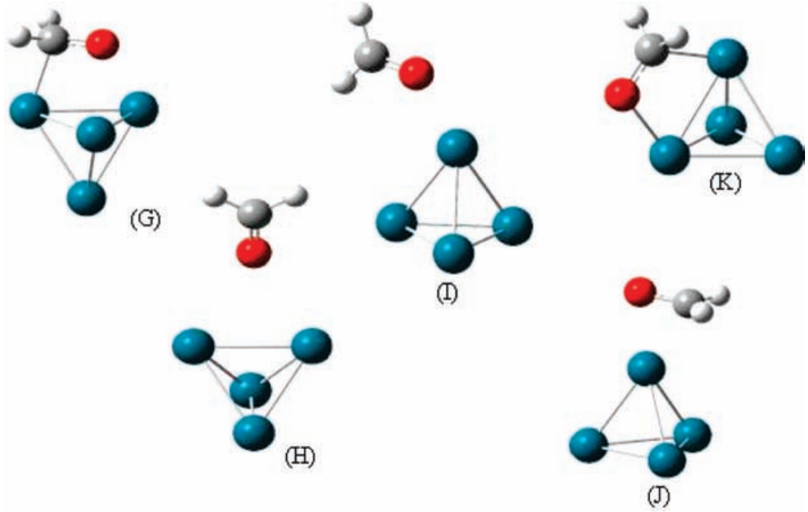

Figure 5. Adsorption forms for formaldehyde adsorption on a tetrahedral Pd_4 cluster.

F)) are at least 4 kcal·mol^{-1} less stable. Although the η^2(C,O)−di-σ arrangement (form B) has a geometry resembling that of A and C, in the B form, the interactions occur with the metal atoms with higher coordination number, therefore leading to lower (less negative) adsorption energy.

The geometry of formaldehyde in the most stable arrangement (A) shows a clear rehybridization of the carbon atom. Geometric parameters (Table 1), such as increased C−O bond length (1.358 Å as compared to 1.241 Å in isolated formaldehyde), reduced H−C−O bond angle (115.9° as compared to 121.9° in isolated formaldehyde), and deviation of the hydrogen atoms from the original molecular plane, as given by the HCOH dihedral angle (20.6°), clearly indicate a high sp^3 character on the carbon atom. Further indication of the degree of deformation in the geometry of formaldehyde as a result of the adsorption process is given by the bond reorganization energy, calculated as the energy difference between the geometry of formaldehyde after adsorption and the full relaxed molecule. For the most stable adsorption form (A), the bond reorganization energy of formaldehyde is 25.3 kcal·mol^{-1}. The smallest C−Pd distance is 2.055 Å, while the smallest O−Pd distance is 2.004 Å. For the arrangements with lower adsorption energy, the changes in the geometric parameters of formaldehyde are correspondingly lower.

Figure 5 gives the geometrical arrangements for the adsorption of formaldehyde over the tetrahedral Pd_4 cluster. The η^2(C,O)−π arrangement (form J) is the most stable with an adsorption energy of −13.2 kcal·mol^{-1}. However, other adsorption forms, such as η^1(O) (form I) and η^2(C,O)−di-σ (form K), are found with only slightly higher energy (less than 3 kcal·mol^{-1}). Although we calculated a higher adsorption energy (more negative) for the planar arrangement of Pd_4, the absolute energy is lower for formaldehyde/Pd_4 tetrahedral than for that

TABLE 2: Adsorption Energy (E_{ad}, kcal·mol^{-1}), Charge Density on Pd_4 (q_t), and Selected Geometrical Parameters for Formaldehyde Adsorbed on Tetrahedral Pd_4 (distances in angstroms and bond angles and dihedral angles in degrees)

	G	H	I	J	K
C−Pd	2.046	4.196	3.078	2.223	2.050
O−Pd	2.185	3.063	2.081	2.194	1.967
C−O	1.397	1.243	1.256	1.319	1.367
C−H	1.101	1.104	1.097	1.082	1.104
H−C−O	113.742	121.742	119.284	118.886	114.493
H−C−O−H	22.68	0.183	0.000	9.045	21.291
E_{ad}[a]	+2.38	+0.07	−11.50	−13.17	−10.23
q_t (Pd_4)	+0.089	−0.107	−0.165	+0.052	+0.152

[a] Adsorption energies were calculated for the triplet state.

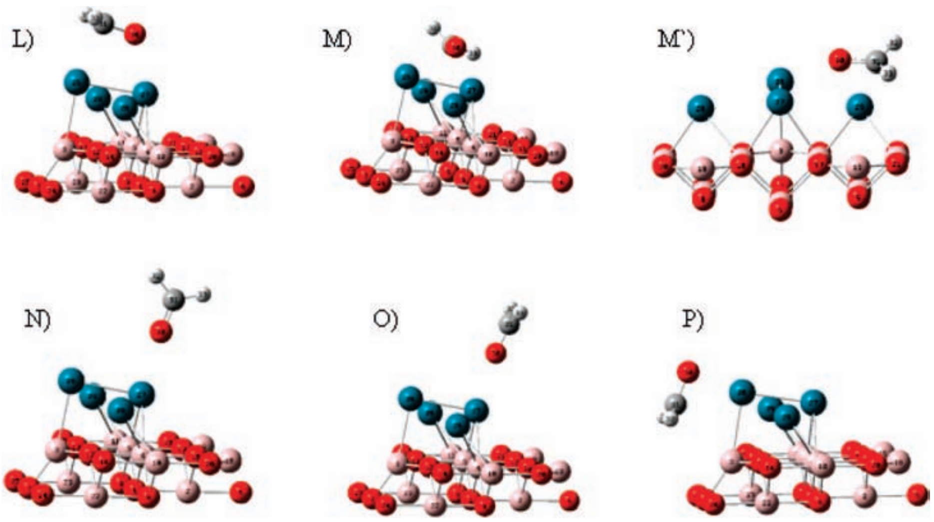

Figure 6. Adsorption forms for adsorption of formaldehyde on the $Pd_4/Al_{10}O_{15}$ cluster. M and M′ are the same adsorption modes shown in different orientations.

formaldehyde/Pd_4 planar, mainly due to the much lower energy of tetrahedral Pd_4 than that of planar Pd_4. Additionally, the lower border effect (due to the higher coordination number) of the tetrahedral Pd_4 cluster makes the adsorption energy lower than that for adsorption on the planar cluster. Therefore, the higher adsorption energy on the tetrahedral cluster compares well with experimental measurements (−12 to −14.6 kcal·mol^{-1}).[34]

Geometrical changes for adsorption on the tetrahedral Pd_4 cluster are smaller than those calculated for planar Pd_4. The C−O bond length increases to 1.319 Å, the H−C−O bond angle decreases to 118.9°, and the dihedral HCOH angle is 9.0° (Table 2). In the most stable arrangement (J), the carbon and oxygen atoms are almost equidistant from the palladium atom in the corner of the tetrahedron (C−Pd = 2.223 Å and O−Pd = 2.194 Å). The bond reorganization energy for formaldehyde adsorbed on the tetrahedral Pd_4 is correspondingly smaller, 10.9 kcal·mol^{-1}. These changes correspond to nearly half of that calculated for adsorption on the planar cluster.

Adsorption of Formaldehyde on $Pd_4/Al_{10}O_{15}$. As a first step in the calculation of the $Pd_4/Al_{18}O_{27}$ ensemble, we fully optimized the geometry of the Pd_4 cluster over the $Al_{18}O_{27}$ cluster. The latter was designed in four layers of Al^{3+} and O^{2-} ions (Figure 3). The four Pd atoms were deposited on the (110C) surface of the $Al_{18}O_{27}$ cluster and were allowed to fully relax while keeping the $Al_{18}O_{27}$ geometry fixed. The final arrangement is shown in Figure 3. Pd_4 adsorbs on the $Al_{18}O_{27}$ cluster in an arrangement which is halfway between the planar and the tetrahedral geometry. After optimization, the palladium atoms are more disperse, with Pd−Pd distances of 3.258 (Pd(x)−Pd(w)), 3.153 (Pd(y)−Pd(w)), and 2.674 Å (Pd(x)−Pd(y) (see Figure 3). Indeed, there are four increased Pd−Pd distances and one reduced Pd−Pd distance. Three of the four palladium atoms (x, w, and z) adsorb in a bridge form involving, in each case, two octahedral aluminum cations, while the fourth Pd atom (y) adsorbs on a tetracoordinated aluminum cation (Figure 3). The smallest Pd−O distances are 2.336 and 2.420 Å, while the smallest Pd−Al distances are 2.489 and 2.567 Å. Among all Pd−Al distances in the metal−alumina interface, those distances inovlving the octahedral aluminum cations (Al_o) are smaller than the distances involving the tetrahedral aluminum cations (Al_t) (Pd(w)−Al_o = 2.498 Å; Pd(w)−Al_o = 2.567 Å; Pd(w)−Al_o = 2.522 Å; Pd(y)−Al_t = 2.590 Å).

After defining the positions of the four palladium atoms on the aluminum cluster, the formaldehyde molecule was adsorbed on the full ensemble Pd_4/alumina. However, in order to reduce computational cost, the two layers farther from the palladium atoms were removed, thereby reducing the size of the alumina cluster from $Al_{18}O_{27}$ to $Al_{10}O_{15}$. The geometry of formaldehyde was then fully optimized over the entire $Pd_4/Al_{10}O_{15}$ ensemble, retaining the geometry of the $Pd_4/Al_{10}O_{15}$ ensemble analogous to that optimized in the previous step. The five main arrangements of formaldehyde adsorbed over the $Pd_4/Al_{10}O_{15}$ ensemble obtained after optimization are given in Figure 6. For all of the adsorption forms shown in Figure 6, the ground electronic spin state is the quintet state. The most stable adsorption form of formaldehyde over the $Pd_4/Al_{10}O_{15}$ ensemble is the η^2(C,O)−π adsorption mode (form M), with an adsorption energy of −12.3 kcal·mol^{-1}. This value is similar to that found for adsorption on the isolated tetrahedral Pd_4 cluster, for the same adsorption mode, and is also close to experimental measurements.[60] A calculation where the first shell of the $Al_{18}O_{27}$ cluster was allowed to relax led to adsorption energy of −16.8 kcal·mol^{-1}, in line with previous calculations.[6] The geometry of adsorbed formaldehyde resembles that calculated for the isolated tetra-

TABLE 3: Adsorption Energy (E_{ad}, kcal·mol^{-1}), Charge Density on Pd$_4$ (q_t), and Selected Geometrical Parameters for Formaldehyde Adsorbed on the Pd$_4$/Al$_{10}$O$_{15}$ Cluster (distances in angstroms and bond angles and dihedral angles in degrees)

	L	M	N	O
C−Pd	2.410	2.118	3.646	3.627
O−Pd	2.293	2.157	2.408	2.391
C−O	1.279	1.325	1.241	1.241
C−H	1.102	1.095	1.103	1.102
H−C−O	120.385	119.268	121.400	121.352
H−C−O−H	7.132	11.239	0.000	0.000
E_{ad}[a]	−3.20	−12.30	−2.29	−2.81
q_t (Pd$_4$)	−1.184	−1.055	−1.202	−1.203

[a] Adsorption energies were calculated for the quintet state.

hedral case, with a C═O bond length of 1.325 Å, H−C−O bond angle of 119.3°, and HCOH dihedral angle of 11.2° (Table 3). This leads to a reorganization energy of 12.5 kcal·mol^{-1}, almost the same value as that calculated for adsorption on the isolated tetrahedral Pd$_4$ cluster. The Pd−O and Pd−C distances are 2.157 and 2.118 Å, respectively. The other adsorption forms are at least 9.1 kcal·mol^{-1} less stable. Therefore, when considering the adsorption of formaldehyde on the supported palladium from the energetic and geometrical point of view, the effect of the Al$_{10}$O$_{15}$ support is not significant. Adsorption energy changes by about 1 kcal·mol^{-1}, and the geometric parameters are essentially the same. The preferred η^2(C,O)−π adsorption form was found in both cases. However, it should be considered that the metal cluster arrangement is not exactly the same in both cases, so that dissimilar effects may compensate and lead to these small differences. For example, while the Pd$_4$ cluster on the alumina surface has a geometry that could lead to a higher adsorption energy, as was observed in the case of the planar Pd$_4$ cluster, the presence of the support, donating an electron to the palladium atoms, therefore decreasing its acidity, as discussed below, may act in the opposite direction, thereby leading to a compensation between these two opposite effects.

Although the additional adsorption forms which were calculated are less stable than the η^2(C,O)−π form, two points regarding their structure caught our attention and may help us understand the nature of the interaction between the aluminum cations and the palladium atoms. The first point is the fact that the π system of formaldehyde moves away from the palladium atom (Pd(27)), which is bonded in a bridge between two octahedral aluminum cations (Al(4) and Al(5)) (see Figure 7 for atom numeration). Upon optimization of this arrangement, the geometry reorganizes in order to allow the oxygen atom to approach the palladium atom, leading to an η^1(O) adsorption form (form O, Figure 6), with a final Pd−O distance of 2.391 Å. The second point was observed when trying to optimize a geometry with the π bond of formaldehyde near to the palladium atom (Pd(26)), which is adsorbed over a tetracoordinated aluminum cation (Al(3)). In this case, optimizations lead to a structure with an η^2(C,O)−di-σ arrangement (form P), however with a tetrahedral aluminum cation as the anchorage point. The first fact is strong evidence of the Lewis acidity of the tetracoordinated aluminum cation, also identified in the NBO analysis (vide infra). The second fact is evidence for some Lewis basicity of the octahedral aluminum cations Al(4) and Al(5), which transfer electrons to the palladium atom. The electron donation effects of the octahedral aluminum cations Al(4) and Al(5) are also seen in the NBO analysis.

In order to verify the effect of fully relaxing the Pd$_4$ arrangement, the η^2(C,O)−π adsorption form was reoptimized, now relaxing not only the geometry of formaldehyde but also the positions of the four palladium atoms. Optimization of both the formaldehyde molecule and the Pd$_4$ cluster over the Al$_{10}$O$_{15}$ cluster reduces the absolute energy by only 1.5 kcal·mol^{-1}, increasing the adsorption energy to −13.8 kcal·mol^{-1}. Geometric changes are also not significant. The only relevant change is the fact that the palladium atom (Pd(26)) adsorbed over the tetracoordinated aluminum cation (Al(3)) moves away, increasing the Pd(26)−Pd(27) distances from 2.674 to 2.721 Å and the Pd(26)−Pd(29) distance from 3.258 to 3.635 Å. This may be an indication of the facility with which the palladium atoms may move over the alumina surface with low energetic cost.

Discussion

The present computational study allows us to derive relevant conclusions about the energetic and geometric parameters for the adsorption of formaldehyde on palladium. Our results clearly indicate that formaldehyde preferentially adsorbs using its π electrons, either in an η^2(C,O)−di-σ adsorption form, where the carbon and oxygen atoms interact each with a palladium atom in a σ-type bond, or in an η^2(C,O)−π adsorption form, where both the carbon and oxygen atoms interact with the same palladium atom in a π-type bond. The first situation was found for the planar arrangement of the Pd$_4$ cluster, while the second was preferentially found in the tetrahedral Pd$_4$ cluster. While both arrangements may compete, more frequently, we found the η^2(C,O)−π adsorption form as the most stable, although the η^2(C,O)−di-σ arrangement was usually only slightly less stable. Adsorption of formaldehyde using the oxygen lone pairs, in an η^1(O) adsorption form, is always much less stable than any of the η^2 adsorption forms discussed above. To our knowledge, no experimental result that could clearly differentiate between the two η^2 adsorption forms has been reported, although experimental evidence suggests the η^2 adsorption form, without differentiation between the σ- and π-bonding possibility. Density functional calculations using extended surfaces based on periodical slabs[29] or more extended flat surfaces[30] lead to the η^2(C,O)−di-σ adsorption form as the most stable. This corresponds to our result using the planar Pd$_4$ cluster, a result that could be expected on the basis of the similarity between the two models. Therefore, it seems that when modeling planar surfaces, using either small clusters or extended surfaces, the η^2(C,O)−di-σ adsorption mode is preferential. However, for a not fully planar arrangement, as is the present case with the tetrahedral cluster model, the η^2(C,O)−π adsorption form may become either competitive or the most stable one.

Intriguingly, we found no remarkable effect of the Al$_{10}$O$_{18}$ support on the adsorption energy of formaldehyde, unless we let the alumina surface relax. On both the isolated (tetrahedral) and the supported Pd$_4$ cluster, the value calculated for the adsorption energy is close to experimental measurements. The geometry of Pd$_4$ deposited on the alumina surface is intermediate between that of the planar and the tetrahedral models. This could lead to adsorption energies that are more negative than that calculated for the isolated tetrahedral model, as was found for the Pd$_4$ cluster in the planar arrangement. However, as will be shown below, the alumina support seems to preferentially transfer electron density to the Pd$_4$ cluster, therefore reducing its acidity and, correspondingly, the adsorption energy. This effect would act in a contrary direction as that predicted on the basis of the geometrical arrangement. Therefore, an imbalance between these two opposite effects may well be responsible for the similarity in the adsorption energies of the isolated and the supported Pd$_4$ clusters. However, the preferred adsorption form

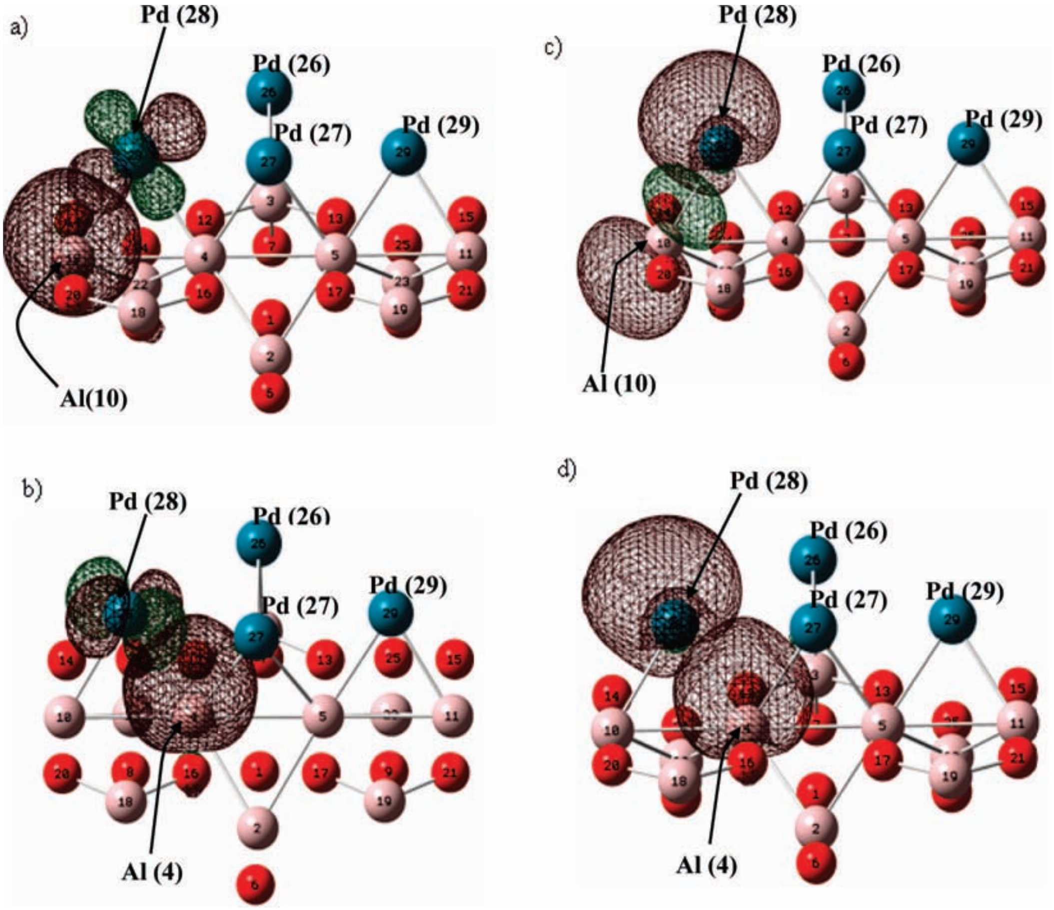

Figure 7. Representation of the NBO orbitals involved in the interaction of Pd(28) with Al(4) and Al(10) octahedral aluminum cations. (a) Back-donation from Pd(28) to Al(10); (b) back-donation from Pd(28) to Al(4); (c) donation from Al(10) to Pd(28); (d) donation from Al(4) to Pd(28).

and geometrical parameters of formaldehyde after adsorption are similar in both situations.

What are the main interactions between the metal and the adsorbate in the present case? Analysis of charge density changes as a consequence of adsorption may help us understand electronic effects acting on the adsorption process. We also carried out NBO calculations, which could help rationalize electron transfer between the metal catalyst and the adsorbate, as well as that between the metal catalyst and the support.

The total Mulliken charge density on the Pd_4 cluster after adsorption of formaldehyde is positive for all adsorption forms, with the exception of those forms where the adsorption involves the oxygen lone pairs (Tables 1, 2, and 3). These are, however, forms with low adsorption energies (as discussed before) and should not be taken into consideration. Charges calculated using the Merz−Kollman−Singh scheme point to the same direction. These results are found for both the η^2(C,O)−di-σ and the η^2(C,O)−π adsorption forms, although with more positive charge on the Pd_4 cluster in the η^2(C,O)−di-σ than in the η^2(C,O)−π adsorption modes. These results may be an indication that back-donation, responsible for electron transfer from the metal d orbitals to the antibonding C═O π orbital, is more relevant than the usual electron donation from the adsorbate to the metal surface. The C═O double bond considerably stretches upon adsorption on either of these modes, which may be a consequence of increased occupation of the antibonding C═O π^* orbital.

The charge density on formaldehyde adsorbed on the $Pd_4/Al_{10}O_{15}$ cluster is negative, with values similar to those calculated for adsorption on the isolated Pd_4 cluster. However, a significant difference is found for the charge density on the four palladium atoms. When they are supported on the $Al_{10}O_{15}$ cluster, the charge density on the metal is negative, with a total charge density on the palladium atoms above $-1e^-$ (Mulliken) or $-0.008e^-$ (Merz−Kollman−Singh). Therefore, even considering the Merz−Kollman−Singh result, there is a relevant charge transfer from the support to the metal catalyst. Individual analysis of charge density on each atom shows that this charge is transferred mainly from the octahedral aluminum atoms with high coordination number to the neighboring palladium atoms. NBO analysis confirms these fact, as the second-order perturbation energy, which gives an indication of the amount of electron transfer between two subunities, is significantly high for interaction between the octahedral aluminum atoms and the palladium atoms directly bonded to them.

NBO analysis for the $Pd_4/Al_{10}O_{15}$ cluster shows that the palladium atoms interact more strongly with the aluminum cations than with the oxygen anions. Figure 7 shows the main orbitals involved in donation and back-donation for the palladium atom (Pd(28) or its symmetrical Pd(29)) adsorbed in a bridge position on the Al(10) and Al(4) aluminum cations. The back-donation interactions involve the $4d_{xy}$ orbital on the palladium atom and a hybrid $sp^{0.52}$ (65.86% s, 34.14% p) valence orbital on the aluminum atom Al(4) as well as the $4d_{xz}$ orbital on the metal and a high s character (90% s and 10% p) orbital localized on the octahedral Al(10) aluminum cation. The second-order perturbation energies for these interactions are 10.1 and 8.9 $kcal \cdot mol^{-1}$, respectively. The donation involves the same

SCHEME 1: HOMO (the highest occupied molecular orbital, either α or *β*) and LUMO (the lowest unoccupied molecular orbital, either α or *β*) Energies for Planar, Distorted, and Tetrahedral Pd_4 Calculated at the UHF/6-31G(d) Level[a]

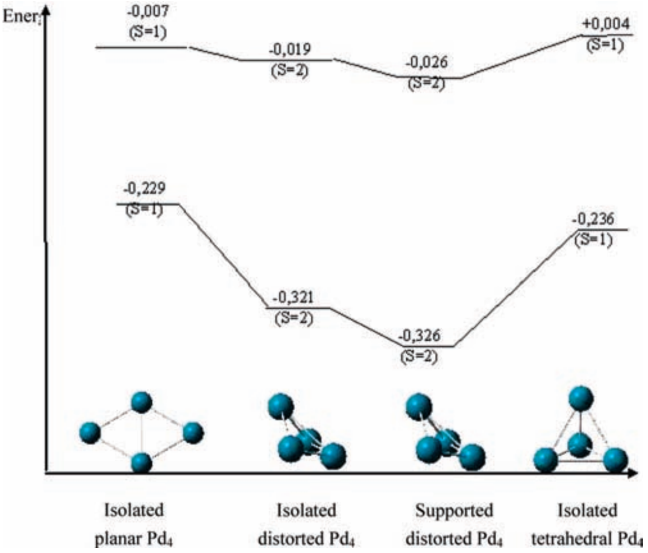

[a] The distorted geometry was obtained from optimization of Pd_4 on the $Al_{18}O_{27}$ cluster. In the second distorted structure (supported Pd_4), the wave functions of $Al_{18}O_{27}$ were included (via ghost atoms).

hybrid orbital on the octahedral aluminum cation (Al(4)), which has a relatively high occupation number ($0.694e^-$) and an s (97.1% s and 1.3% p) orbital on the palladium atom as well as a p (92.5% p and 7.5% s) orbital on Al(10). The second-order perturbation energies for these donation interactions are 23.4 and 18.1 kcal·mol^{-1}, respectively. Although the second-order perturbation energy for the individual interactions is higher for donation than it is for back-donation, when taking all of the interactions together, that is, including interactions between other orbitals, the total back-donation is 21.5 kcal·mol^{-1} stronger than the donation. This is probably associated with the fact that the aluminum atom has low coordination number, therefore forcing strong back-donation from the metal. Corresponding interactions were also found for the palladium atom (Pd(27)) deposited over the octahedral aluminum atoms Al(4) and Al(5). Nevertheless, in this case, donation is stronger than back-donation. For adsorption on the tetracoordinated aluminum cation (Al(3)), the backdonation interactions involve the d_{z^2} orbital on Pd(26) and an $sp^{0.45}$ (68.7% s and 31.2% p) hybrid orbital on the aluminum cation. The NBO result indicates reduction in the occupation of the d_{z^2} orbital ($1.821e^-$) and increased occupation of the $sp^{0.45}$ orbital ($0.439e^-$). The second-order perturbation energy for this interaction is 19.8 kcal·mol^{-1}. No noteworthy interaction corresponding to a classical donation was found. In summary, the NBO results indicate that the tetrahedral aluminum atoms behave as a Lewis acid, given that only back-donation interactions were found in this case. In contrast, the octahedral aluminum atoms, at least those of high coordination number, may act as a Lewis base and may donate electrons to the metal support.

The energy of the HOMO and LUMO orbitals of the Pd_4 cluster may also help understand the origin of donation and back-donation in the interaction between the Pd_4 cluster and the alumina support. The HOMO and LUMO energies for the planar, tetrahedral, and two distorted arrangements of the Pd_4 cluster are given in Scheme 1. The distorted geometry of Pd_4 is that optimized over the alumina support. Calculations for the distorted Pd_4 were carried out in the absence and in the presence of the alumina support (using ghost atoms to represent the alumina basis sets). The orbital energies were calculated with the unrestricted Hartree−Fock model using the 6-31G(d) basis set.

The results show that the HOMO energy of the supported palladium cluster is 0.097 eV lower than the corresponding energy for the isolated (tetrahedral) cluster. This reduction comes mainly from the change in the geometry of the cluster, with a small contribution due to the alumina wave functions. Similar reduction in energy upon distortion of the tetrahedral arrangement is also calculated for the LUMO orbitals. For the supported Pd_4, the LUMO energy is 0.030 eV lower than the LUMO energy of the tetrahedral cluster and 0.020 eV lower than the LUMO energy of the planar cluster. In this case, the aluminum wave functions are responsible for 0.007 eV in the reduction of the LUMO energy of the distorted Pd_4. Reduction of the energies of the frontier orbitals may be the origin for the increased charge transfer from the support to the metal cluster. While lower HOMO energies preclude electron donation from the metal to the alumina cluster (back-donation), a corresponding lowering in the LUMO energy of Pd_4 helps donation from the alumina to the Pd_4 cluster. This is reflected in the electron transfer from the alumina to the metal, as discussed above.

Conclusions

In the present work, we report a detailed analysis of the adsorption forms and adsorption energies for formaldehyde adsorbed on small palladium clusters and palladium supported on an $Al_{10}O_{15}$ cluster. Our calculations suggest that the η^2 adsorption forms, where the π electrons of the carbon−oxygen double bond interact with the metal surface, either in a σ-type or in a π-type bonding arrangement, are more stable than the alternative bonding through the oxygen lone pairs. For the planar Pd_4 cluster, the preferential adsorption form is the η^2(C,O)−di-σ mode, while for adsorption on the tetrahedral Pd_4 cluster, the η^2(C,O)−π mode is favored. The calculated adsorption energies for these two adsorption forms are −21.4 and −13.2 kcal·mol^{-1}, respectively. Although the adsorption energy is higher (more negative) for the planar cluster, the absolute energy for adsorption on the tetrahedral cluster is smaller. Therefore, the last should be considered as the most stable species. The corresponding adsorption energy is close to experimental measurements (−12 to −14 kcal·mol^{-1}). Adsorption on Pd_4 supported on the $Al_{10}O_{15}$ cluster changes neither the energy nor the preferential adsorption form when compared to the adsorption on the tetrahedral cluster, although the geometry of the supported Pd_4 is intermediate between that of the tetrahedral and the planar clusters.

Charge density analysis indicates that electronic charge density is transferred from the metal to formaldehyde when it adsorbs on the Pd_4 cluster in either of the η^2 adsorption modes. In the presence of alumina, not only the charge on the formaldehyde but also that on the metal becomes negative as a result of charge transfer from alumina to the metal cluster. This is a consequence of the strong reduction in the LUMO energy of the distorted Pd_4 when adsorbed on the alumina surface. NBO analysis indicates that this charge transfer involves mainly the highly coordinated octahedral aluminum atoms, which act as Lewis bases, donating electronic charge to the metal cluster, in opposition to the lower coordinated tetrahedral aluminum atoms, which behave as Lewis acids and are electron acceptors.

Acknowledgment. J.W.d.M.C. received a research fellowship from CNPq. M.T.d.M.C. has a graduate fellowship from CAPES. Financial support was given by CNPq (Grant 477611/2006-0) and FAPERJ (Grant E-26/152.786/2006).

References and Notes

(1) Somorjai, G. A. *Introduction to Surface Chemistry and Catalysis*; Wiley-Interscience: New York, 1994; p 450.

(2) Argo, A. M.; Odzak, J. F.; Gates, B. C. *J. Am. Chem. Soc.* **2003**, *125*, 7107.

(3) Argo, A. M.; Odzak, J. F.; Goellner, J. F.; Lai, F. S.; Xiao, F.-S.; Gates, B. C. *J. Phys. Chem. B* **2006**, *110*, 175.

(4) Ferrari, A. M.; Neyman, K. M.; Mayer, M.; Staufer, M.; Gates, B. C.; Rosch, N. *J. Phys. Chem. B* **1999**, *103*, 5311.

(5) Argo, A. M.; Goellner, J. F.; Phillips, B. L.; Panjabi, G. A.; Gates, B. C. *J. Am. Chem. Soc.* **2001**, *123*, 2275.

(6) Gomes, J. R. B.; Lodziana, Z.; Illas, F. *J. Phys. Chem. B* **2003**, *107*, 6411.

(7) Argo, A. M.; Odzak, J. F.; Lai, F. S.; Gates, B. C. *Nature* **2002**, *415*, 623.

(8) Dropsch, H.; Baerns, M. *Appl. Catal., A* **1997**, *158*, 163.

(9) Chang, J. R.; Chang, S.-L.; Lin, T.-B. *J. Catal.* **1997**, *169*, 338.

(10) Baumgarten, E.; Weinstrauch, F.; Höffkes, H. *J. Chromatogr.* **1977**, *138*, 347.

(11) Neumann, M. G. *J. Chem. Educ.* **1976**, *53*, 708.

(12) Bravo, M.; Fuertes, A. B.; Coca, J. *React. Kinet. Catal. Lett.* **1986**, *31*, 173.

(13) Thielmann, F.; Baumgarten, E. *J. Colloid Interface Sci.* **2000**, *229*, 418.

(14) Cai, S.; Sohlberg, K. *J. Mol. Catal.* **2003**, *193*, 157.

(15) Raybaud, P.; Costa, D.; Corral Valero, M.; Arrouvel, C.; Digne, M.; Sautet, P.; Toulhoat, H. *J. Phys.: Condens. Matter* **2008**, *20*, 064235.

(16) Peri, J. B. *J. Phys. Chem.* **1965**, *69*, 220.

(17) Knozinger, H.; Ratnasamy, P. *Catal. Rev. Sci. Eng.* **1978**, *17*, 31.

(18) Tanabe, K. *Solid Acids and Bases: Their Catalytic Properties*; Academic Press: New York, 1970.

(19) De Vito, D. A.; Gilardoni, F.; Kiwi-Minsker, L.; Morgantini, P.-Y.; Porchet, S.; Renken, A.; Weber, J. *J. Mol. Struct.: THEOCHEM* **1999**, *469*, 7.

(20) Díaz, E.; Ordóñez, S.; Veja, A.; Coca, J. *Microporous Mesoporous Mater.* **2004**, *70*, 109.

(21) Ealet, B.; Gillet, E. *Surf. Sci.* **1996**, *367*, 221.

(22) Ogawa, S.; Ichikawa, S. *Phys. Rev. B* **1995**, *51*, 17231.

(23) Matolín, V.; Stará, I.; Tsud, N.; Johánek, V. *Prog. Surf. Sci.* **2001**, *67*, 167.

(24) Marguez, A. M.; Sanz, J. F. *Appl. Surf. Sci.* **2004**, *238*, 82.

(25) Mavrikakis, M.; Barteau, M. A. *J. Mol. Catal. A* **1998**, *131*, 135.

(26) Chetty, N.; Weinert, M.; Rahman, T. S.; Davenport, J. W. *Phys. Rev. B* **1995**, *52*, 6313.

(27) Davis, J. L.; Barteau, M. A. *Surf. Sci.* **1992**, *268*, 11.

(28) Delbecq, F.; Sautet, P. *J. Catal.* **2002**, *211*, 398.

(29) Gomes, J. R. B.; Gomes, J.; Illas, F. *J. Mol. Catal. A: Chem.* **2001**, *170*, 187.

(30) Desai, S. K.; Neurock, M.; Kourtakis, K. *J. Phys. Chem. B* **2002**, *106*, 2559.

(31) Neurock, M. *Top. Catal.* **1999**, *9*, 135.

(32) Schennach, R.; Eichler, A.; Rendulic, K. D. *J. Phys. Chem. B* **2003**, *107*, 2552.

(33) Greeley, J.; Mavrikakis, M. *J. Am. Chem. Soc.* **2002**, *124*, 7193.

(34) Davis, J. L.; Barteau, M. A. *J. Am. Chem. Soc.* **1989**, *111*, 1782.

(35) Kua, J.; Goddard, G. A., III. *J. Am. Chem. Soc.* **1999**, *121*, 10928.

(36) Delbecq, F.; Sautet, P. *Surf. Sci.* **1993**, *295*, 353.

(37) Lide, D. R. *CRC Handbook of Chemistry and PhysicsBoca*, 77th ed. Ed.; CRC: Raton, FL, 1996; Chapter 12, p 18.

(38) Saeys, M.; Reyniers, M.-F.; Marin, G. B.; Neurock, M. *J. Phys. Chem. B* **2002**, *106*, 7489.

(39) Bertin, V.; Agacino, E.; López-Rendon, R.; Poulain, E. *J. Mol. Struct.: THEOCHEM* **2006**, *769*, 243.

(40) Letardi, S.; Cleri, F. *J. Chem. Phys.* **2004**, *120*, 10062.

(41) Van Santen, R. A. *J. Mol. Catal. A: Chem.* **1996**, *107*, 5.

(42) Becke, A. D. *J. Chem. Phys.* **1992**, *96*, 2155.

(43) Lee, C.; Yang, W.; Parr, R. G. *Phys. Rev. B* **1988**, *37*, 785.

(44) Hay, P. J.; Wadt, W. R. *J. Chem. Phys.* **1985**, *82*, 270.

(45) Dunning, T. H., Jr.; Hay, P. J. In *Modern Theoretical Chemistry*; Schaefer, H. F., III, Ed.; Plenum: New York, 1976; Vol. 3, pp 1−28.

(46) Hehre, W. J.; Ditchfield, R.; Pople, J. A. *J. Chem. Phys.* **1972**, *56*, 2257.

(47) Álvarez, L. J.; Fernández Sanz, J.; Capitán, M. J.; Centeno, M. A.; Odriozola, J. A. *J. Chem. Soc., Faraday Trans.* **1989**, *89*, 3623.

(48) Maresca, O. *J. Mol. Struct.: THEOCHEM* **2003**, *620*, 119.

(49) Wyckoff, R. W. G. *Crystal Structures*; Interscience: NewYork, 1968; Vol. 2.

(50) Maroto-Valiente, A.; Rodríguez-Ramos, I.; Guerrero-Ruiz, A. *Thermochim. Acta* **2001**, *379*, 195.

(51) Cruz, M. T. d. M.; Carneiro, J. W. d. M.; Aranda, D. A. G.; Buhl, M. *J. Phys. Chem. C* **2007**, *111*, 11068.

(52) Singh, U. C.; Kollman, P. A. *J. Comput. Chem.* **1984**, *5*, 129.

(53) Besler, B. H.; Merz, K. M., Jr.; Kollman, P. A. *J. Comput. Chem.* **1990**, *11*, 431.

(54) Morokuma, K. *J. Chem. Phys.* **1970**, *19*, 553.

(55) Mulliken, R. S. *J. Chem. Phys.* **1955**, *23*, 1833.

(56) Frisch, M. J. Trucks, G. W.; Schlegel, H. B.; Scuseria, G. E.; Robb, M. A.; Cheeseman, J. R.; Montgomery, J. A., Jr.; Vreven, T.; Kudin, K. N.; Burant, J. C.; Millam, J. M.; Iyengar, S. S.; Tomasi, J.; Barone, V.; Mennucci, B.; Cossi, M.; Scalmani, G.; Rega, N.; Petersson, G. A.; Nakatsuji, H.; Hada, M.; Ehara, M.; Toyota, K.; Fukuda, R.; Hasegawa, J.; Ishida, M.; Nakajima, T.; Honda, Y.; Kitao, O.; Nakai, H.; Klene, M.; Li, X.; Knox, J. E.; Hratchian, H. P.; Cross, J. B.; Bakken, V.; Adamo, C.; Jaramillo, J.; Gomperts, R.; Stratmann, R. E.; Yazyev, O.; Austin, A. J.; Cammi, R.; Pomelli, C.; Ochterski, J. W.; Ayala, P. Y.; Morokuma, K.; Voth, G. A.; Salvador, P.; Dannenberg, J. J.; Zakrzewski, V. G.; Dapprich, S.; Daniels, A. D.; Strain, M. C.; Farkas, O.; Malick, D. K.; Rabuck, A. D.; Raghavachari, K.; Foresman, J. B.; Ortiz, J. V.; Cui, Q.; Baboul, A. G.; Clifford, S.; Cioslowski, J.; Stefanov, B. B.; Liu, G.; Liashenko, A.; Piskorz, P.; Komaromi, I.; Martin, R. L.; Fox, D. J.; Keith, T.; Al-Laham, M. A.; Peng, C. Y.; Nanayakkara, A.; Challacombe, M.; Gill, P. M. W.; Johnson, B.; Chen, W.; Wong, M. W.; Gonzalez, C.; Pople, J. A. *Gaussian 03*, revision B.04; Gaussian, Inc.: Pittsburgh, PA, 2003.

(57) Dai, D.; Balasubramanian, K. *J. Chem. Phys.* **1995**, *103*, 648.

(58) Zacarias, A. G.; Castro, M.; Tour, J. M.; Seminario, J. M. *J. Phys. Chem. A* **1999**, *103*, 7692.

(59) Estiu, G. L.; Zerner, M. C. *J. Phys. Chem.* **1994**, *98*, 4793.

(60) Goursot, A.; Papai, I.; Salahub, D. R. *J. Am. Chem. Soc.* **1992**, *114*, 7452.

(61) Valerio, G.; Toulhout, H. *J. Phys. Chem.* **1996**, *100*, 10827.

(62) Moc, J.; Musaev, D. G.; Morokuma, K. *J. Phys. Chem. A* **2000**, *104*, 11606.

(63) Balasubramanian, K. *J. Chem. Phys.* **1989**, *91*, 307.

(64) Balasubramanian, K. *J. Chem. Phys.* **1995**, *103*, 648.

(65) Valero, M. C.; Raybaud, P.; Sautet, P. *J. Catal.* **2007**, *247*, 339.

JP801591Z